

Three-dimensional atrial wall thickness maps to inform catheter ablation procedures for atrial fibrillation

Martin Bishop¹, Ronak Rajani^{1,2,3}, Gernot Plank^{4,5}, Nicholas Gaddum¹, Gerry Carr-White^{1,2,3}, Matt Wright^{1,3}, Mark O'Neill^{1,3*}, and Steven Niederer¹

¹Department of Imaging Sciences and Biomedical Engineering King's College London, London SE1 7EH, UK; ²Department of Cardiac Computed Tomography, Guy's and St Thomas' NHS Foundation Trust, London SE1 7EH, UK; ³Department of Cardiology, Guy's and St Thomas' NHS Foundation Trust, London SE1 7EH, UK; ⁴Institute of Biophysics, Medical University of Graz, Graz, Austria; and ⁵Oxford e-Research Centre, University of Oxford, Oxford, UK

Received 15 January 2015; accepted after revision 3 March 2015; online publish-ahead-of-print 4 April 2015

Aims

Transmural lesion formation is critical to success in atrial fibrillation ablation and is dependent on left atrial wall thickness (LAWT). Pre- and peri-procedural planning may benefit from LAWT measurements.

Methods and results

To calculate the LAWT, the Laplace equation was solved over a finite element mesh of the left atrium derived from the segmented computed tomographic angiography (CTA) dataset. Local LAWT was then calculated from the length of field lines derived from the Laplace solution that spanned the wall from the endocardium or epicardium. The method was validated on an atrium phantom and retrospectively applied to 10 patients who underwent routine coronary CTA for standard clinical indications at our institute. The Laplace wall thickness algorithm was validated on the left atrium phantom. Wall thickness measurements had errors of <0.2 mm for thicknesses of 0.5–5.0 mm that are attributed to image resolution and segmentation artefacts. Left atrial wall thickness measurements were performed on 10 patients. Successful comprehensive LAWT maps were generated in all patients from the coronary CTA images. Mean LAWT measurements ranged from 0.6 to 1.0 mm and showed significant inter and intra patient variability.

Conclusions

Left atrial wall thickness can be measured robustly and efficiently across the whole left atrium using a solution of the Laplace equation over a finite element mesh of the left atrium. Further studies are indicated to determine whether the integration of LAWT maps into pre-existing 3D anatomical mapping systems may provide important anatomical information for guiding radiofrequency ablation.

Keywords

Cardiac computed tomography • Left atrial wall thickness • Atrial fibrillation • Finite element modelling • Ablation • Mapping

Introduction

Atrial fibrillation (AF) is a prevalent and progressive condition associated with increased morbidity and mortality. Isolation of the pulmonary veins via radiofrequency ablation (RFA) offers effective treatment of symptoms in drug refractory symptomatic patients with paroxysmal AF. However, long-term success rates of ablation procedures remain suboptimal with many patients requiring multiple procedures.

Left atrial wall thickness (LAWT) is likely to be an important parameter in determining procedural success from RFA. The thickness

of the left atrial wall is related not only to the risk of cardiac perforation and tamponade following ablation^{1,2} but also to the success rates in achieving effective transmural lesions. Furthermore, LAWT has been shown to predict the transition from paroxysmal to persistent AF,³ be associated with complex fractionated electrograms,⁴ and to influence the behaviour of rotor activation patterns⁵ that may identify suitable ablation targets for patients with both paroxysmal and persistent AF.⁶

Despite these potential benefits, the measurement of LAWT poses a number of challenges. The morphology and regional wall thickness of the left atrium is highly variable and in the presence of

* Corresponding author. Tel: +44 020 7188 4989; fax: +44 020 7188 5442, E-mail address: mark.oneill@kcl.ac.uk

Published on behalf of the European Society of Cardiology. All rights reserved. © The Author 2015. For permissions please email: journals.permissions@oup.com.

What's new?

- We describe and demonstrate a protocol for segmenting out the atrial myocardium tissue from contrast cardiac computed tomography images.
- We have developed a robust and automated algorithm for calculating maps of atrial wall thickness across the entirety of the left atrium.
- The wall thickness algorithm is validated using on a 3D printed atrial phantom.
- The ability to calculate the left atrial wall thickness maps across the atrium is demonstrated in 10 patient cases.

AF, there is an implicit need for an imaging technique with both a high temporal and spatial resolution to be able to measure the LAWTT reliably. These factors are largely accountable for the absence of any routine approach for measuring LAWTT in clinical practice. The primary aim of this study was to determine whether the application of an image derived finite element method could be used to provide a reliable semi-automated technique for providing a LAWTT map of the entire left atrial surface in patients undergoing routine coronary computed tomographic angiography (CTA). The secondary aim was to validate this approach for measuring LAWTT using a 3D printed left atrium phantom.

Methods

As part of this feasibility study, we retrospectively analysed 10 consecutive patients who underwent clinically indicated coronary CTA at Guy's and St Thomas' NHS Foundation Trust from January 2013 through July 2013. Patients were excluded if they had a prior history of mechanical aortic or mitral valve implantation, permanent pacemaker implantation, AF with a ventricular rate > 120 b.p.m., a BMI > 35 , and if their image quality was not considered adequate for clinical interpretation. All patients underwent detailed analysis of their coronary arteries for clinical purposes, followed by an assessment of LAWTT using a freely available

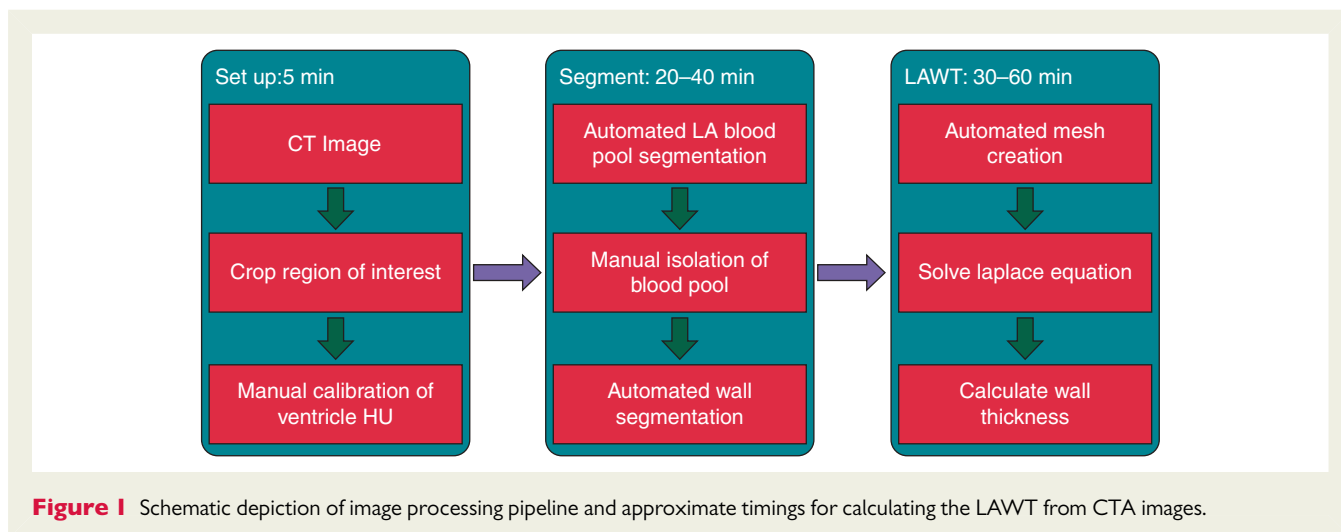
segmentation tools package and a finite element-based method, as detailed below.

Coronary computed tomographic angiography image acquisition and reconstruction

Coronary CTA was performed on a Philips 256 iCT scanner (Philips Healthcare, Amsterdam, Netherlands). Beta-blockade with intravenous metoprolol was used to achieve a heart rate of < 65 b.p.m. for those patients in sinus rhythm and < 100 b.p.m. for patients in AF. All patients received 0.8 mg of sublingual nitroglycerin spray 3–5 min prior to the scan acquisition to dilate the coronary arteries. Following adequate heart rate control, 90 mL of intravenous contrast (Omnipaque; GE Healthcare, Princeton, NJ, USA), followed by 90 mL of a 35%:65% contrast to saline mix, and 20 mL of a saline chaser, at a rate of 6 mL/s were power-injected into the antecubital vein. Descending aorta contrast-triggered (120 HU), ECG-gated scanning was then performed in a single breath hold. Scanning parameters included heart rate dependent pitch (0.2–0.45), gantry rotation time of 270 ms, tube voltage of 100 or 120 kVp, depending on the patient's BMI and a tube current of 125–300 mA s depending on the thoracic circumference measurement. Where the heart rate was < 65 b.p.m. a step and shoot acquisition with 3% phase tolerance was acquired. For patients with heart rates > 65 b.p.m., a retrospective ECG-gated acquisition was acquired to permit ECG-editing and reconstruction of additional systolic phases. The acquired coronary CTA data were reconstructed using iterative reconstruction (iDose level 4) with the use of 0.8 mm slice thickness, 0.4 mm slice increment, 250 mm field of view, 512×512 matrix, and a sharp reconstruction kernel. If reconstruction from standard phases of the cardiac cycle resulted in left atrial wall boundaries that were marred by cardiac motion artefact, additional phases were reconstructed and analysed. In the presence of significant ventricular ectopy, ECG-editing was performed using vendor-specific software.

Calculating left atrial wall thickness

The calculation of LAWTT involved three stages, shown schematically in Figure 1. The first stage required the cropping of the CT image to isolate the atria. The second stage involved the segmentation of the left atrium from the entire cardiac CTA dataset, whilst the third stage



involved solving the Laplace equations over a computational model generated from the respective segmented left atrium.

Segmentation

Creating a segmentation of the atria from any imaging modality is an essential part of calculating wall thickness. Images were segmented using the Python scripting tools for automating image processing steps within the freely available Seg3D2 software package.⁷ In brief, coronary CTA scans were manually cropped to encapsulate the left atria. An automated script applied a 4-point median filter to the image and segmented the left atrial blood cavity using a threshold value of 250 HU. The blood pool threshold was manually corrected to remove spurious connections with the aorta, coronary sinus, and right atria. A sphere was placed in the left ventricle that identified the location of the mitral valve, and separated any labelled ventricular blood from the left atrial blood pool. An automated script then identified all viable atrial myocardial tissue. First, regions with 50–180 HU (this elevated value reflects the presence of contrast agent in the blood elevating the HU value of myocardium) were thresholded. These values were chosen based on the HU values of the left ventricular myocardium. Large thick contiguous regions were removed from the mask of potential atrial tissue, due to the undesired inclusion of the un-contrasted right atrial blood pool and basal left ventricular tissue. The atrial blood pool, identified previously, was then removed from the reduced mask to identify all viable regions of atrial tissue. The atrial wall was then segmented in layers. The first layer was formed by dilating the blood pool region by 1 voxel as the atrial wall was assumed to be at least 1 voxel thick. The remaining layers were determined by dilating the current atrial wall and adding any regions that fell on voxels labelled previously as being viable atrial tissue. This was repeated four times. The final image was then dilated and eroded by 2 voxels to remove any spurious segmentations.

Solving the Laplace equations

At its simplest wall thickness can be calculated by the length of the normal projection (Figure 2A) from either the endocardial (point x) or epicardial (point y) surface or the shortest Euclidian distance between the two surfaces at any two points (Figure 2B).

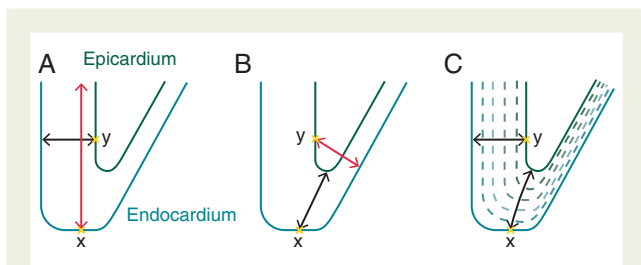


Figure 2 Schematic showing different approaches for measuring atrial wall thickness between the endocardium (turquoise surface) and epicardium (green surface). (A) Left atrial wall thickness calculated using a normal projection from the surface generates a spurious result at point x (red arrow). (B) Left atrial wall thickness calculated using a nearest point on the opposing surface generates a spurious result for point y. (C) The Laplace method calculates smooth dashed lines between the endocardium and epicardium. Paths that are orthogonal to these lines (black arrows) are used to calculate the wall thickness removing the spurious results observed in the normal projection and nearest point approaches.

However, as demonstrated in Figure 2, these approaches can generate spurious solutions, as indicated by the red arrows. From electromagnetism we know that by solving the Laplace equation we can derive a smooth set of non-intersecting field lines between two bodies, be they points, lines, sheets, or arbitrary objects. As shown in Figure 2C, a family of dashed curves can be created that provide smooth, non-intersecting, and continuous lines between the surfaces. The distance of curves orthogonal to these lines, then provides a measure of the wall thickness at all points on the endocardial and epicardial surface. The length of the field lines is calculated in three steps.

First the Laplace equation,

$$\nabla^2 u = 0 \quad (1)$$

is solved over the domain (Ω) encompassing the atrial wall, enclosed by the endocardial ($\partial\Omega_{\text{endo}}$), epicardial ($\partial\Omega_{\text{epi}}$), and remaining ($\partial\Omega_r$) boundary surfaces. We impose boundary conditions

$$\begin{aligned} u|_{\partial\Omega_{\text{epi}}} &= 1 \\ u|_{\partial\Omega_{\text{endo}}} &= 0 \\ \frac{\partial u}{\partial n}|_{\partial\Omega_r} &= 0. \end{aligned} \quad (2)$$

In brief, Eq. (1) is solved using the finite element simulation platform Cardiac Arrhythmia Research Package.^{8,9} High fidelity and resolution tetrahedral meshes are created over the atrial wall using the Tarantula meshing software package (www.meshing.az) to mathematically define the atrial wall domain (Ω). Unstructured tetrahedral meshes are used to allow subvoxel resolution and remove potential bias in the solution from regular voxel-based meshes. The nodes lying on the edge of the cropped segmentation image and within 1 mm of the sphere defining the mitral valve are labelled as belonging to the remaining boundary surface ($\partial\Omega_r$). A flood fill algorithm is then used to identify all unconnected node groups that lie on the mesh surface. The first and second largest node groups are then set as the epicardium and endocardium, respectively. All other surface nodes are labelled as lying on the remaining boundary surface.

Calculating the length of field lines

To calculate the LAWTF from the Laplace equations requires the calculation of field lines and the subsequent integration of length along the field lines. The field line direction at each element in the finite element mesh is calculated from

$$v = \frac{\nabla u}{\|\nabla u\|}. \quad (3)$$

To calculate the length of field line particles is seeded on the endocardium and epicardium. The particles move away from their initial surface in the direction of the vector field (Eq. 3). Tracking the distance travelled by a particle as it traverses from the endocardium to epicardium or vice versa then gives the wall thickness at the point of the particle's origin.

Left atrium phantom

A left atrium phantom was created to validate the Laplace wall thickness method applied to CT images. The phantom was designed to test the accuracy of the wall thickness measurements and determine the limits of the method within the resolution constraints of CT. The model was created in Solidworks and printed using a 100 μm resolution resin 3D printer. The model was scanned using the cardiac CT protocol with an ECG emulator.

Computation and visualization

All results were performed using a 12 core Xeon X5650 2.67 GHz Linux Dell work station with 40 Gb of memory. Meshes and all results were visualized using Meshalyzer courtesy of Dr E. J. Vigmond.

Results

Algorithm validation

Figure 3 shows the left atrium phantom design (Figure 3A) and the 3D printed phantom and corresponding CT image (Figure 3B). Figure 3C and D compares the wall thickness calculation directly from the design and from the CT image of phantom, respectively. Figure 3E compares the error in wall thickness calculations for the computer design (top row) and from the CT image (bottom row). The known thicknesses of each of the eight segments of the left atrium phantom are labelled 0.25, 0.5, 1.0, 1.5, 2.0, 3.0, 4.0, and 5.0 mm between the rows. The pulmonary vein-like structures have thicknesses of 0.5 and 1.0 mm. Greyed out and white regions have error beyond 0.2 mm. In regions close to the insertion of pulmonary vein-like structure, we see a significant grey area corresponding to the thinning of the segment at the point of insertion; this is most prominent in the 5 mm segment.

The top panel of Figure 3E quantifies the error introduced by the discretization of the phantom volume, solution of the Laplace equations, and calculation of stream line length. The error is on the order of <0.05 mm this compares with a mesh mean resolution of 0.125 mm.

The bottom panel of Figure 3E shows the ability of the Laplace method to calculate wall thickness from CT images. For wall thicknesses >0.5 mm, the error falls within 0.2 mm. For thickness of 0.25 and 0.5 mm, the error is >0.2 mm. We can see from the top panel of Figure 3E that given an idealized description of the geometry

that the Laplace method is capable of accurately calculating these thicknesses, but that for thicknesses of <0.5 mm the resolution of the CT image and the effect of partial volumes on the segmentation mean that the Laplace method cannot quantitatively determine the wall thickness.

Calculation of wall thickness across the atria

There were 10 patients with a median age of 51 (32–86) years of whom 4 were male. Coronary CTA was performed as a prelude to cardiothoracic surgery in 5 (50%) patients, for symptoms of chest pain in 4 (40%) patients and to exclude left atrial appendage thrombus in 1 (10%) patient. Of the 10 patients 8 (80%) were in sinus rhythm and 2 (20%) patients in AF at the time of the scan. The baseline demographics for the population are given in Table 1.

Ten atria were segmented providing voxel-based descriptions of atrial anatomy, taking ~ 30 min per case. The steps of the segmentation process are shown in Figure 4. Tetrahedral meshes were created for all atria taking ~ 20 min. Figure 5 shows an example mesh and level of detail captured by the mesh. Mean mesh edge length was 0.18–0.27 mm with 1.9–4.1 million and 9.4–20.6 million degrees of freedom and tetrahedral per mesh, respectively.

The Laplace equation was solved for each case taking ~ 30 s. The gradient was then calculated as a post-processing step and used to calculate field line lengths directly using particle tracking taking ~ 30 min. Figure 6 shows the calculated wall thickness on the endocardium and epicardium for the 10 cases. We see the algorithm correctly identifying thicker protrusions on the atria surface and a range of thickness distributions between patients with some cases having notably thicker walls across the roof of the atria. The resulting distribution of wall thickness for each patient case is shown in Figure 7.

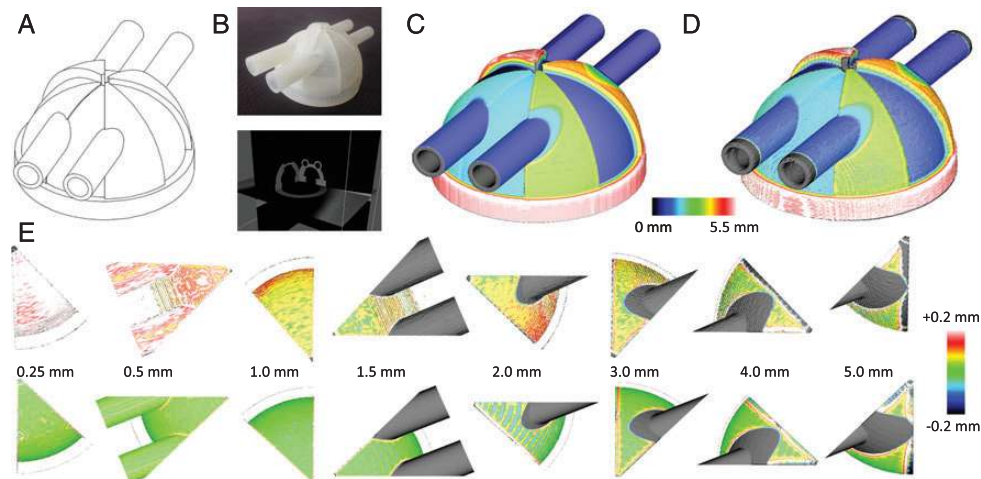


Figure 3 Validation of Laplace wall thickness method. (A) Schematic of computed model of the left atrium phantom. (B) Three-dimensional printed and CT images from the atrium phantom. (C) Wall thickness calculated from the computer model of the atrium phantom. (D) Wall thickness calculated from the CT image of the 3D printed atrium phantom. (E) Comparison of the error in each wall segment against the known true value for the computer modelled atrium (top row) and the CT image of the 3D printed phantom (bottom row).

Table 1 Baseline demographics

Age (years)	51 (32–86)
Gender (M:F)	4:6
Smoking history, <i>n</i> (%)	3 (30%)
Cardiovascular risk factors	
Hypercholesterolemia, <i>n</i> (%)	2 (20%)
Hypertension, <i>n</i> (%)	4 (40%)
Positive family history, <i>n</i> (%)	2 (20%)
Diabetes mellitus, <i>n</i> (%)	0 (0%)
Atrial fibrillation, <i>n</i> (%)	2 (20%)
Coronary CTA indication	
Chest pain, <i>n</i> (%)	4 (40%)
Prelude to cardiothoracic surgery, <i>n</i> (%)	5 (50%)
Left atrial appendage thrombus, <i>n</i> (%)	1 (%)
Coronary CTA scan mode	
Prospective, <i>n</i> (%)	8 (80%)
Retrospective, <i>n</i> (%)	2 (20%)
Mean heart rate (b.p.m.)	61 (\pm 12)
Total dose length product (mGy cm)	415 (\pm 338)
Peak tube voltage (kVp)	116 (\pm 8)
Tube current (mA)	511 (\pm 141)

Discussion

In the present study we validate and apply for the first time a novel tool chain to robustly calculate LAWТ across the entire left atrium.

Atrial fibrillation is the most common sustained arrhythmia with an estimated overall prevalence of 0.95%.¹⁰ It is associated with significant morbidity and mortality from stroke, sudden cardiac death, heart failure, and impaired cognitive function.^{11,12} Although pulmonary vein isolation by RFA has emerged as an effective treatment for carefully selected symptomatic patients, the long-term success rates remain suboptimal with repeated procedures often being required. It is possible that the incorporation of LAWТ measurements into pre-procedural planning and intra-procedural guidance may be useful in improving patient outcomes by identifying thin high-risk locations, identifying ablation targets and permitting titration of RF energy and contact force according to site- and patient-specific structural characteristics.

Despite these potential benefits, the measurement of LAWТ is challenging. There is a high degree of left atrial anatomical variability with individual patients having atria with a distinct size, shape, and number of pulmonary veins.¹³ In addition, the walls of the atria consist of multiple tissue types, with distinct physiology, roles, and properties. The left atrial wall predominantly consists of atrial myocytes but also contains fibrous and fatty tissue that make up an important component of the total wall thickness.¹⁴ The significant variation in wall thickness across the atria, the lack of a unique repeatable anatomic reference system, and ambiguity in the definition of wall thickness leads to significant variation in reported wall thickness measurements for different methodologies and patient populations.^{15–20} Previous direct measurements of atrial wall thickness have been performed *ex vivo* in cadaveric anatomical studies.^{15,16}

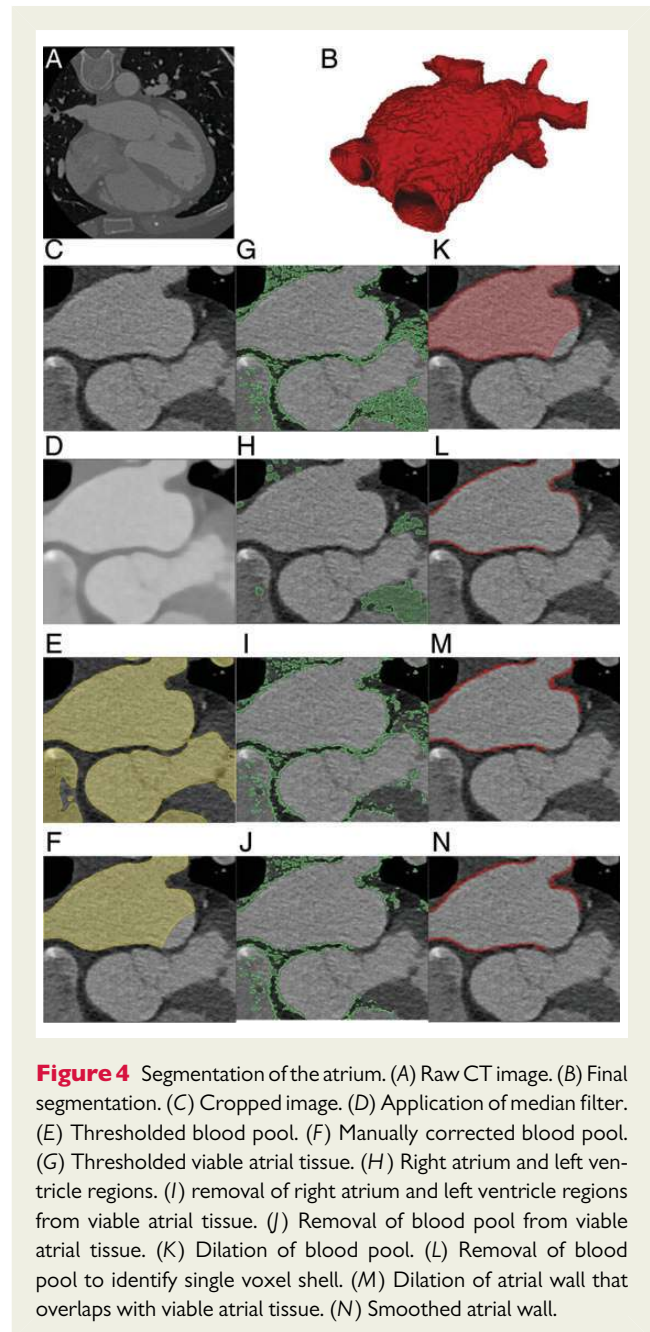


Figure 4 Segmentation of the atrium. (A) Raw CT image. (B) Final segmentation. (C) Cropped image. (D) Application of median filter. (E) Thresholded blood pool. (F) Manually corrected blood pool. (G) Thresholded viable atrial tissue. (H) Right atrium and left ventricle regions. (I) removal of right atrium and left ventricle regions from viable atrial tissue. (J) Removal of blood pool from viable atrial tissue. (K) Dilatation of blood pool. (L) Removal of blood pool to identify single voxel shell. (M) Dilatation of atrial wall that overlaps with viable atrial tissue. (N) Smoothed atrial wall.

These measurements were performed at discrete locations and may have included varying amounts of fatty or fibrous tissue in the thickness measurements. The results from these two studies are discrepant: atrial thickness was measured at 2.1–2.9 mm across the roof of the atria in one study¹⁵ but was more than 50% thinner with a mean roof thickness of 1.06 mm in a second study.¹⁶ Variation in thickness between atrial regions has also been observed in CT studies of the left atrium,¹⁵ which reveal consistently smaller wall thicknesses when compared with cadaveric studies. This may reflect the limited resolution of CT measurements due to voxel size in earlier studies, that CT differentiates myocardium from fat and hence different tissue fractions are included in the measurement¹⁷ or, that the fixation process affects measurements. In studies that have measured

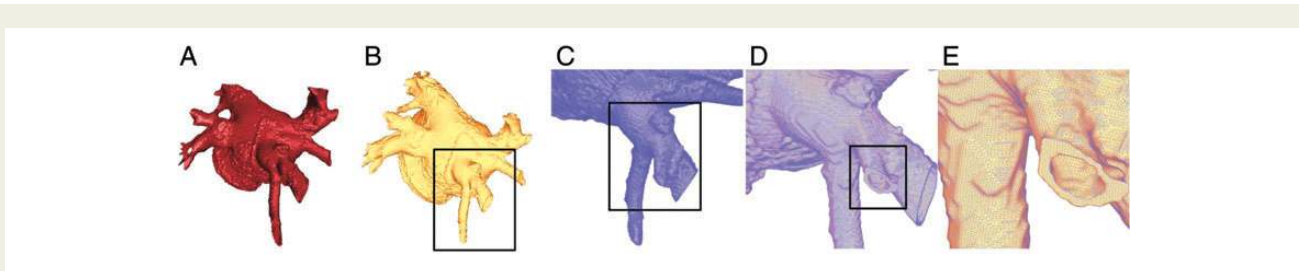


Figure 5 Atria (A) segmentation and corresponding (B) mesh. Increasing zoom of mesh resolution is shown in (C)–(E).

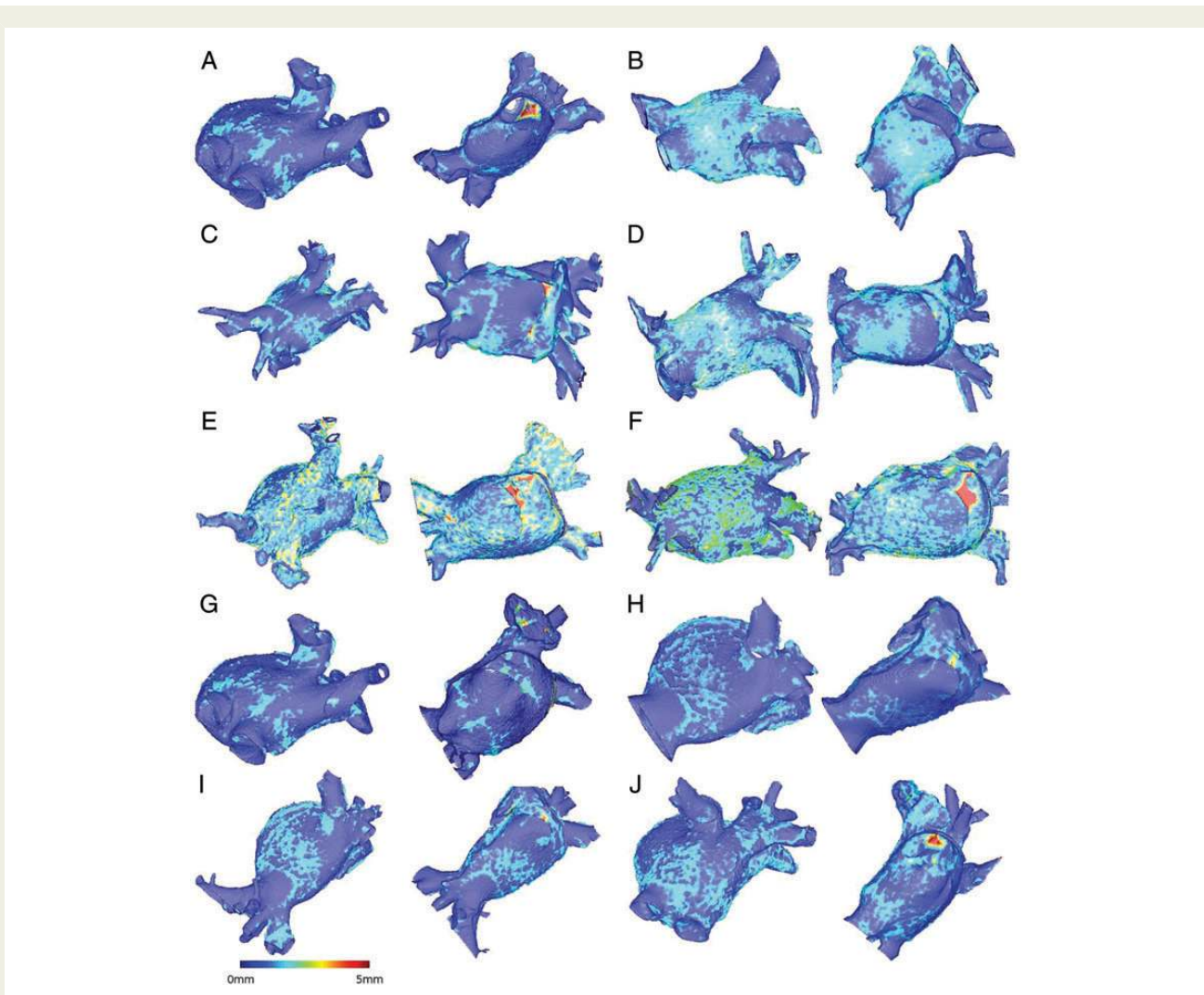
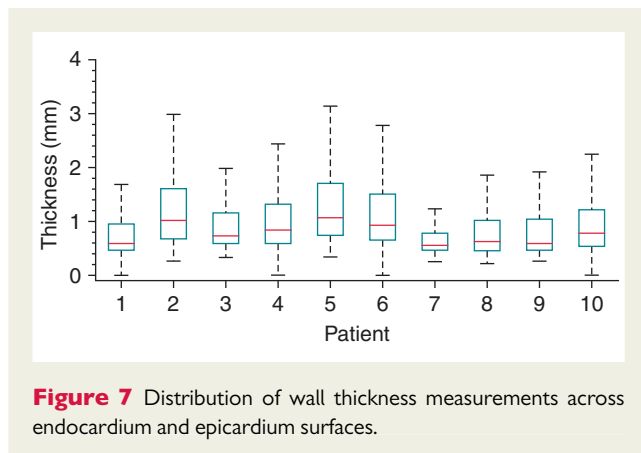


Figure 6 Endocardial and epicardial wall thickness from 0 mm (dark blue) to 5 mm (red) for patients 1–10 (A–J), respectively.

LAWT along lines of ablation in patients with AF, there has been considerable variability with measurements varying from 2.1–2.9 mm¹⁸ to 0–7.7 mm.¹⁹ This significant variation both between patients and across different regions of the atria motivates the need to measure regional wall thickness in individuals.

There are a number of limitations to previously reported techniques for measuring LAW. In *ex vivo* fixed preparations of the left atrium, the measurements of LAW using calipers likely included fibrotic, fat, and myocardial tissue. In addition, it is recognised that there is variability in LAW measurements at different sites of the



atrium. This renders isolated *ex vivo* or *in vivo* measurements of LAWTT unreliable in describing the complex non-homogenous wall thickness of the left atrium. These limitations validate the need for a technique that can rapidly and accurately generate LAWTT maps that can be utilized clinically.

In the present study we therefore developed a novel technique to efficiently and effectively improve LAWTT measurements using a finite element-based method. The Laplace equation was solved on a finite element mesh of the atria and the length of the field lines running from the endocardium to the epicardium provided a complete description of the atrial wall thickness. We separated this process into three modular components that will permit further refinements with evolving technology. First, we describe a simple semi-automated, yet robust, method for segmenting the atrial wall. Secondly, we generate a high-quality finite element tetrahedral mesh and solve the Laplace equations. Thirdly, the lengths of the field lines were calculated. In this study we focused on describing and validating the tool chain. Further studies are indicated to determine whether the incorporation of LAWTT maps into pre- or peri-procedural RFCA procedures for AF will result in improved patient outcomes.

Limitations

This study represents a feasibility and methodology study and hence the patient numbers are small. We elected to include patients in both sinus rhythm and AF to ensure that the technique was robust across different patient populations. Although we demonstrate that the measurement of LAWTT is possible using mathematical modelling, the findings in this study were not used clinically. Further studies are indicated to determine whether the incorporation of LAWTT maps from patients in AF impact on pre- or peri-procedural planning and post-procedural outcomes from RFA. This is the subject of ongoing work by our group.

Clinical implementation

There is increasing interest in calculating LAWTT for clinical studies and guiding procedures. We have demonstrated a robust and accurate method for calculating LAWTT in the complex LA anatomy. The current implementation is an offline processing pipeline that takes 1.5–2 h. This time could be reduced to 45–60 min by implementing

a fully automated segmentation and parallelising the particle tracking elements of the code could. The LAWTT calculations are dependent on the CTA image and subsequent segmentation quality. Tailoring the CTA protocol to maximize contrast in both the RA and LA chambers would improve identification of the atrial septum and calculation of its thickness.

Conclusion

The measurement of LAWTT can be reliably performed and displayed using the solution of the Laplace equations in patients with sinus rhythm and AF. The thin sheet approximation greatly reduces the computational and implementation burden for calculating wall thickness while only introducing nominal errors in the wall thickness calculation. Further work is indicated to determine whether the incorporation of LAWTT measurements improves outcomes and procedural success in patients undergoing RFA for AF.

Funding

S.A.N. is supported by the British Heart Foundation (PG/11/101/29212). The authors acknowledge financial support from the National Institute for Health Research (NIHR) comprehensive Biomedical Research Centre award to Guy's & St Thomas' NHS Foundation Trust. G.P. is supported by the Austrian Science Fund FWF (F3210-N18). The funders had no role in study design, data collection and analysis, decision to publish, or preparation of the manuscript.

Conflict of interest: none declared.

References

- Cappato R, Calkins H, Chen S-A, Davies W, Iesaka Y, Kalman J *et al*. Prevalence and causes of fatal outcome in catheter ablation of atrial fibrillation. *J Am Coll Cardiol* 2009; **53**:1798–803.
- Bunch TJ, Asirvatham SJ, Friedman PA, Monahan KH, Munger TM, Rea RF *et al*. Outcomes after cardiac perforation during radiofrequency ablation of the atrium. *J Cardiovasc Electrophysiol* 2005; **16**:1172–9.
- Nakamura K, Funabashi N, Uehara M, Ueda M, Murayama T, Takaoka H *et al*. Left atrial wall thickness in paroxysmal atrial fibrillation by multislice-CT is initial marker of structural remodeling and predictor of transition from paroxysmal to chronic form. *Int J Cardiol* 2011; **148**:139–47.
- Park J, Park CH, Lee H-J, Wi J, Uhm J-S, Pak H-N *et al*. Left atrial wall thickness rather than epicardial fat thickness is related to complex fractionated atrial electrogram. *Int J Cardiol* 2014; **172**:e411–3.
- Yamazaki M, Mironov S, Taravant C, Brec J, Vaquero LM, Bandaru K *et al*. Heterogeneous atrial wall thickness and stretch promote scroll waves anchoring during atrial fibrillation. *Cardiovasc Res* 2012; **94**:48–57.
- Narayan SM, Krummen DE, Shivkumar K, Clopton P, Rappel W-J, Miller JM. Treatment of Atrial Fibrillation by the Ablation of Localized Sources: CONFIRM (Conventional Ablation for Atrial Fibrillation With or Without Focal Impulse and Rotor Modulation) Trial. *J Am Coll Cardiol* 2012; **60**:628–36.
- Institute S-Cal. "Seg3D" volumetric image segmentation and visualization. Scientific Computing and Imaging Institute (SCI). <http://www.seg3d.org/last> accessed.
- Vigmond EJ, Hughes M, Plank G, Leon LJ. Computational tools for modeling electrical activity in cardiac tissue. *J Electrocardiol* 2003; **36**:69–74.
- Niederer S, Mitchell L, Smith N, Plank G. Simulating human cardiac electrophysiology on clinical time-scales. *Front Physiol* 2011; **2**:14.
- Go AS, Hylek EM, Phillips KA, Chang Y, Henault LE, Selby JV *et al*. Prevalence of diagnosed atrial fibrillation in adults: national implications for rhythm management and stroke prevention: the AnTicoagulation and Risk Factors in Atrial Fibrillation (ATRIA) Study. *JAMA* 2001; **285**:2370–5.
- Benjamin EJ, Wolf PA, D'Agostino RB, Silbershatz H, Kannel WB, Levy D. Impact of atrial fibrillation on the risk of death: the Framingham Heart Study. *Circulation* 1998; **98**:946–52.
- Stewart S, Hart CL, Hole DJ, McMurray JJV. A population-based study of the long-term risks associated with atrial fibrillation: 20-year follow-up of the Renfrew/Paisley study. *Am J Med* 2002; **113**:359–64.

13. Ho SY, Sánchez-Quintana D. The importance of atrial structure and fibers. *Clin Anat* 2009;**22**:52–63.
14. Sánchez-Quintana D, Cabrera JA, Climent V, Farré J, de Mendonça MC, Ho SY. Anatomic relations between the esophagus and left atrium and relevance for ablation of atrial fibrillation. *Circulation* 2005;**112**:1400–5.
15. Platonov PG, Ivanov V, Ho SY, Mitrofanova L. Left atrial posterior wall thickness in patients with and without atrial fibrillation: data from 298 consecutive autopsies. *J Cardiovasc Electrophysiol* 2008;**19**:689–92.
16. Hall B, Jeevanantham V, Simon R, Filippone J, Vorobiof G, Daubert J. Variation in left atrial transmural wall thickness at sites commonly targeted for ablation of atrial fibrillation. *J Interv Card Electrophysiol* 2006;**17**:127–32.
17. Beinat ROY, Abbara S, Blum A, Ferencik M, Heist K, Ruskin J *et al*. Left atrial wall thickness variability measured by CT scans in patients undergoing pulmonary vein isolation. *J Cardiovasc Electrophysiol* 2011;**22**:1232–6.
18. Cho Y, Lee W, Park E-A, Oh I-Y, Choi E-K, Seo J-W *et al*. The anatomical characteristics of three different endocardial lines in the left atrium: evaluation by computed tomography prior to mitral isthmus block attempt. *Europace* 2012;**14**:1104–11.
19. Becker AE. Left atrial isthmus. *J Cardiovasc Electrophysiol* 2004;**15**:809–12.
20. Park YM, Park HC, Ban JE, Choi JJ, Lim HE, Park SW *et al*. Interatrial septal thickness is associated with the extent of left atrial complex fractionated atrial electrograms and acute procedural outcome in patients with persistent atrial fibrillation. *Europace* 2015;**17**:1700–7.

EP CASE EXPRESS

doi:10.1093/europace/euv407

Online publish-ahead-of-print 30 December 2015

Mitral isthmus ablation: the importance of epicardial connections between the coronary sinus and Marshall bundle

Takekuni Hayashi*, Takeshi Mitsuhashi, and Shin-ichi Momomura

Division of Cardiovascular Medicine, Saitama Medical Center, Jichi Medical University, 1-847, Amanuma, Oomiya-ku, Saitama 330-8503, Japan

*Corresponding author. Tel: +81 48 647 2111; fax: +81 48 647 5188. E-mail address: hayashi1979@yahoo.co.jp

The ligament of Marshall is an epicardial vestigial fold that contains the vein of Marshall (VOM) and a myocardial sleeve called the Marshall bundle (MB). Marshall bundle epicardial connections bypassing the endocardial mitral isthmus (MI) should be blocked to achieve complete MI block. We report the first instance of MB conduction block through disconnection of coronary sinus (CS)–MB connections.

A 47-year-old man underwent ablation for persistent atrial fibrillation. An epicardial conduction pathway via the MB bypassing endocardial MI was suspected, and a 2 Fr octapolar electrode was inserted into the VOM. After the endocardial MI and CS ablation, the VOM activation sequence during CS 7–8 pacing changed from proximal to distal to proximal. The conduction time from CS 1–2 to VOM 1–2 during CS 1–2 pacing was longer than that from CS 7–8 to VOM 1–2 during CS 7–8 pacing. The conduction time from VOM 3–4 to CS 7–8 during VOM 3–4 pacing was also longer than that from VOM 1–2 to CS 7–8 during VOM 1–2 pacing. These findings indicated the complete bidirectional block of CS–MB connections. Close attention should be paid to the MB epicardial connections, whereby complete MI block may be successfully achieved without excess radiofrequency application.

The full-length version of this report can be viewed at: <http://www.escardio.org/Guidelines-&Education/E%E2%80%93learning/Clinical-cases/Electrophysiology/EP-Case-Reports>

